

Search for particles decaying into a Z boson and a photon in $p\bar{p}$ collisions at $\sqrt{s} = 1.96$ TeV

V.M. Abazov,³⁶ B. Abbott,⁷⁶ M. Abolins,⁶⁶ B.S. Acharya,²⁹ M. Adams,⁵² T. Adams,⁵⁰ M. Agelou,¹⁸ J.-L. Agram,¹⁹ S.H. Ahn,³¹ M. Ahsan,⁶⁰ G.D. Alexeev,³⁶ G. Alkhazov,⁴⁰ A. Alton,⁶⁵ G. Alverson,⁶⁴ G.A. Alves,² M. Anastasoae,³⁵ T. Andeen,⁵⁴ S. Anderson,⁴⁶ B. Andrieu,¹⁷ M.S. Anzels,⁵⁴ Y. Arnoud,¹⁴ M. Arov,⁵³ A. Askew,⁵⁰ B. Åsman,⁴¹ A.C.S. Assis Jesus,³ O. Atramentov,⁵⁸ C. Autermann,²¹ C. Avila,⁸ C. Ay,²⁴ F. Badaud,¹³ A. Baden,⁶² L. Bagby,⁵³ B. Baldin,⁵¹ D.V. Bandurin,⁵⁹ P. Banerjee,²⁹ S. Banerjee,²⁹ E. Barberis,⁶⁴ P. Bargassa,⁸¹ P. Baringer,⁵⁹ C. Barnes,⁴⁴ J. Barreto,² J.F. Bartlett,⁵¹ U. Bassler,¹⁷ D. Bauer,⁴⁴ A. Bean,⁵⁹ M. Begalli,³ M. Begel,⁷² C. Belanger-Champagne,⁵ L. Bellantoni,⁵¹ A. Bellavance,⁶⁸ J.A. Benitez,⁶⁶ S.B. Beri,²⁷ G. Bernardi,¹⁷ R. Bernhard,⁴² L. Berntzon,¹⁵ I. Bertram,⁴³ M. Besançon,¹⁸ R. Beuselinck,⁴⁴ V.A. Bezzubov,³⁹ P.C. Bhat,⁵¹ V. Bhatnagar,²⁷ M. Binder,²⁵ C. Biscarat,⁴³ K.M. Black,⁶³ I. Blackler,⁴⁴ G. Blazey,⁵³ F. Blekman,⁴⁴ S. Blessing,⁵⁰ D. Bloch,¹⁹ K. Bloom,⁶⁸ U. Blumenschein,²³ A. Boehnlein,⁵¹ O. Boeriu,⁵⁶ T.A. Bolton,⁶⁰ F. Borchering,⁵¹ G. Borissov,⁴³ K. Bos,³⁴ T. Bose,⁷⁸ A. Brandt,⁷⁹ R. Brock,⁶⁶ G. Brooijmans,⁷¹ A. Bross,⁵¹ D. Brown,⁷⁹ N.J. Buchanan,⁵⁰ D. Buchholz,⁵⁴ M. Buehler,⁸² V. Buescher,²³ S. Burdin,⁵¹ S. Burke,⁴⁶ T.H. Burnett,⁸³ E. Busato,¹⁷ C.P. Buszello,⁴⁴ J.M. Butler,⁶³ P. Calfayan,²⁵ S. Calvet,¹⁵ J. Cammin,⁷² S. Caron,³⁴ W. Carvalho,³ B.C.K. Casey,⁷⁸ N.M. Cason,⁵⁶ H. Castilla-Valdez,³³ S. Chakrabarti,²⁹ D. Chakraborty,⁵³ K.M. Chan,⁷² A. Chandra,⁴⁹ D. Chapin,⁷⁸ F. Charles,¹⁹ E. Cheu,⁴⁶ F. Chevallier,¹⁴ D.K. Cho,⁶³ S. Choi,³² B. Choudhary,²⁸ L. Christofek,⁵⁹ D. Claes,⁶⁸ B. Clément,¹⁹ C. Clément,⁴¹ Y. Coadou,⁵ M. Cooke,⁸¹ W.E. Cooper,⁵¹ D. Coppage,⁵⁹ M. Corcoran,⁸¹ M.-C. Cousinou,¹⁵ B. Cox,⁴⁵ S. Crépe-Renaudin,¹⁴ D. Cutts,⁷⁸ M. Ćwiok,³⁰ H. da Motta,² A. Das,⁶³ M. Das,⁶¹ B. Davies,⁴³ G. Davies,⁴⁴ G.A. Davis,⁵⁴ K. De,⁷⁹ P. de Jong,³⁴ S.J. de Jong,³⁵ E. De La Cruz-Burelo,⁶⁵ C. De Oliveira Martins,³ J.D. Degenhardt,⁶⁵ F. Déliot,¹⁸ M. Demarteau,⁵¹ R. Demina,⁷² P. Demine,¹⁸ D. Denisov,⁵¹ S.P. Denisov,³⁹ S. Desai,⁷³ H.T. Diehl,⁵¹ M. Diesburg,⁵¹ M. Doidge,⁴³ A. Dominguez,⁶⁸ H. Dong,⁷³ L.V. Dudko,³⁸ L. Dufлот,¹⁶ S.R. Dugad,²⁹ A. Duperrin,¹⁵ J. Dyer,⁶⁶ A. Dyshkant,⁵³ M. Eads,⁶⁸ D. Edmunds,⁶⁶ T. Edwards,⁴⁵ J. Ellison,⁴⁹ J. Elmsheuser,²⁵ V.D. Elvira,⁵¹ S. Eno,⁶² P. Ermolov,³⁸ J. Estrada,⁵¹ H. Evans,⁵⁵ A. Evdokimov,³⁷ V.N. Evdokimov,³⁹ S.N. Fatakia,⁶³ L. Felgioni,⁶³ A.V. Ferapontov,⁶⁰ T. Ferbel,⁷² F. Fiedler,²⁵ F. Filthaut,³⁵ W. Fisher,⁵¹ H.E. Fisk,⁵¹ I. Fleck,²³ M. Ford,⁴⁵ M. Fortner,⁵³ H. Fox,²³ S. Fu,⁵¹ S. Fuess,⁵¹ T. Gadfort,⁸³ C.F. Galea,³⁵ E. Gallas,⁵¹ E. Galyaev,⁵⁶ C. Garcia,⁷² A. Garcia-Bellido,⁸³ J. Gardner,⁵⁹ V. Gavrilov,³⁷ A. Gay,¹⁹ P. Gay,¹³ D. Gelé,¹⁹ R. Gelhaus,⁴⁹ C.E. Gerber,⁵² Y. Gershtein,⁵⁰ D. Gillberg,⁵ G. Gintler,⁷² N. Gollub,⁴¹ B. Gómez,⁸ K. Gounder,⁵¹ A. Goussiou,⁵⁶ P.D. Grannis,⁷³ H. Greenlee,⁵¹ Z.D. Greenwood,⁶¹ E.M. Gregores,⁴ G. Grenier,²⁰ Ph. Gris,¹³ J.-F. Grivaz,¹⁶ S. Grünendahl,⁵¹ M.W. Grünewald,³⁰ F. Guo,⁷³ J. Guo,⁷³ G. Gutierrez,⁵¹ P. Gutierrez,⁷⁶ A. Haas,⁷¹ N.J. Hadley,⁶² P. Haefner,²⁵ S. Hagopian,⁵⁰ J. Haley,⁶⁹ I. Hall,⁷⁶ R.E. Hall,⁴⁸ L. Han,⁷ K. Hanagaki,⁵¹ K. Harder,⁶⁰ A. Harel,⁷² R. Harrington,⁶⁴ J.M. Hauptman,⁵⁸ R. Hauser,⁶⁶ J. Hays,⁵⁴ T. Hebbeker,²¹ D. Hedin,⁵³ J.G. Hegeman,³⁴ J.M. Heinmiller,⁵² A.P. Heinson,⁴⁹ U. Heintz,⁶³ C. Hensel,⁵⁹ G. Hesketh,⁶⁴ M.D. Hildreth,⁵⁶ R. Hirosky,⁸² J.D. Hobbs,⁷³ B. Hoeneisen,¹² H. Hoeth,²⁶ M. Hohlfeld,¹⁶ S.J. Hong,³¹ R. Hooper,⁷⁸ P. Houben,³⁴ Y. Hu,⁷³ Z. Hubacek,¹⁰ V. Hynek,⁹ I. Iashvili,⁷⁰ R. Illingworth,⁵¹ A.S. Ito,⁵¹ S. Jabeen,⁶³ M. Jaffré,¹⁶ S. Jain,⁷⁶ K. Jakobs,²³ C. Jarvis,⁶² A. Jenkins,⁴⁴ R. Jesik,⁴⁴ K. Johns,⁴⁶ C. Johnson,⁷¹ M. Johnson,⁵¹ A. Jonckheere,⁵¹ P. Jonsson,⁴⁴ A. Juste,⁵¹ D. Käfer,²¹ S. Kahn,⁷⁴ E. Kajfasz,¹⁵ A.M. Kalinin,³⁶ J.M. Kalk,⁶¹ J.R. Kalk,⁶⁶ S. Kappler,²¹ D. Karmanov,³⁸ J. Kasper,⁶³ P. Kasper,⁵¹ I. Katsanos,⁷¹ D. Kau,⁵⁰ R. Kaur,²⁷ R. Kehoe,⁸⁰ S. Kermiche,¹⁵ S. Kesisoglou,⁷⁸ N. Khalatyan,⁶³ A. Khanov,⁷⁷ A. Kharchilava,⁷⁰ Y.M. Kharzheev,³⁶ D. Khatidze,⁷¹ H. Kim,⁷⁹ T.J. Kim,³¹ M.H. Kirby,³⁵ B. Klima,⁵¹ J.M. Kohli,²⁷ J.-P. Konrath,²³ M. Kopal,⁷⁶ V.M. Korablev,³⁹ J. Kotcher,⁷⁴ B. Kothari,⁷¹ A. Koubarovsky,³⁸ A.V. Kozelov,³⁹ J. Kozminski,⁶⁶ A. Kryemadhi,⁸² S. Krzywdzinski,⁵¹ T. Kuhl,²⁴ A. Kumar,⁷⁰ S. Kunori,⁶² A. Kupco,¹¹ T. Kurča,^{20,*} J. Kvita,⁹ S. Lager,⁴¹ S. Lammers,⁷¹ G. Landsberg,⁷⁸ J. Lazoflores,⁵⁰ A.-C. Le Bihan,¹⁹ P. Lebrun,²⁰ W.M. Lee,⁵³ A. Leflat,³⁸ F. Lehner,⁴² V. Lesne,¹³ J. Leveque,⁴⁶ P. Lewis,⁴⁴ J. Li,⁷⁹ Q.Z. Li,⁵¹ J.G.R. Lima,⁵³ D. Lincoln,⁵¹ J. Linnemann,⁶⁶ V.V. Lipaev,³⁹ R. Lipton,⁵¹ Z. Liu,⁵ L. Lobo,⁴⁴ A. Lobodenko,⁴⁰ M. Lokajicek,¹¹ A. Lounis,¹⁹ P. Love,⁴³ H.J. Lubatti,⁸³ M. Lynker,⁵⁶ A.L. Lyon,⁵¹ A.K.A. Maciel,² R.J. Madaras,⁴⁷ P. Mättig,²⁶ C. Magass,²¹ A. Magerkurth,⁶⁵ A.-M. Magnan,¹⁴ N. Makovec,¹⁶ P.K. Mal,⁵⁶ H.B. Malbouisson,³ S. Malik,⁶⁸ V.L. Malyshev,³⁶ H.S. Mao,⁶ Y. Maravin,⁶⁰ M. Martens,⁵¹ S.E.K. Mattingly,⁷⁸ R. McCarthy,⁷³ R. McCroskey,⁴⁶ D. Meder,²⁴ A. Melnitchouk,⁶⁷ A. Mendes,¹⁵ L. Mendoza,⁸ M. Merkin,³⁸ K.W. Merritt,⁵¹ A. Meyer,²¹ J. Meyer,²²

M. Michaut,¹⁸ H. Miettinen,⁸¹ T. Millet,²⁰ J. Mitrevski,⁷¹ J. Molina,³ N.K. Mondal,²⁹ J. Monk,⁴⁵ R.W. Moore,⁵ T. Moulik,⁵⁹ G.S. Muanza,¹⁶ M. Mulders,⁵¹ M. Mulhearn,⁷¹ L. Mundim,³ Y.D. Mutaf,⁷³ E. Nagy,¹⁵ M. Naimuddin,²⁸ M. Narain,⁶³ N.A. Naumann,³⁵ H.A. Neal,⁶⁵ J.P. Negret,⁸ S. Nelson,⁵⁰ P. Neustroev,⁴⁰ C. Noeding,²³ A. Nomerotski,⁵¹ S.F. Novaes,⁴ T. Nunnemann,²⁵ V. O'Dell,⁵¹ D.C. O'Neil,⁵ G. Obrant,⁴⁰ V. Oguri,³ N. Oliveira,³ N. Oshima,⁵¹ R. Otec,¹⁰ G.J. Otero y Garzón,⁵² M. Owen,⁴⁵ P. Padley,⁸¹ N. Parashar,⁵⁷ S.-J. Park,⁷² S.K. Park,³¹ J. Parsons,⁷¹ R. Partridge,⁷⁸ N. Parua,⁷³ A. Patwa,⁷⁴ G. Pawloski,⁸¹ P.M. Perea,⁴⁹ E. Perez,¹⁸ K. Peters,⁴⁵ P. Pétroff,¹⁶ M. Petteni,⁴⁴ R. Piegai,¹ M.-A. Pleier,²² P.L.M. Podesta-Lerma,³³ V.M. Podstavkov,⁵¹ Y. Pogorelov,⁵⁶ M.-E. Pol,² A. Pompoš,⁷⁶ B.G. Pope,⁶⁶ A.V. Popov,³⁹ W.L. Prado da Silva,³ H.B. Prosper,⁵⁰ S. Protopopescu,⁷⁴ J. Qian,⁶⁵ A. Quadt,²² B. Quinn,⁶⁷ K.J. Rani,²⁹ K. Ranjan,²⁸ P.A. Rapidis,⁵¹ P.N. Ratoff,⁴³ P. Renkel,⁸⁰ S. Reucroft,⁶⁴ M. Rijssenbeek,⁷³ I. Ripp-Baudot,¹⁹ F. Rizatdinova,⁷⁷ S. Robinson,⁴⁴ R.F. Rodrigues,³ C. Royon,¹⁸ P. Rubinov,⁵¹ R. Ruchti,⁵⁶ V.I. Rud,³⁸ G. Sajot,¹⁴ A. Sánchez-Hernández,³³ M.P. Sanders,⁶² A. Santoro,³ G. Savage,⁵¹ L. Sawyer,⁶¹ T. Scanlon,⁴⁴ D. Schaile,²⁵ R.D. Schamberger,⁷³ Y. Scheglov,⁴⁰ H. Schellman,⁵⁴ P. Schieferdecker,²⁵ C. Schmitt,²⁶ C. Schwanenberger,⁴⁵ A. Schwartzman,⁶⁹ R. Schwienhorst,⁶⁶ S. Sengupta,⁵⁰ H. Severini,⁷⁶ E. Shabalina,⁵² M. Shamim,⁶⁰ V. Shary,¹⁸ A.A. Shchukin,³⁹ W.D. Shephard,⁵⁶ R.K. Shivpuri,²⁸ D. Shpakov,⁶⁴ V. Siccaldi,¹⁹ R.A. Sidwell,⁶⁰ V. Simak,¹⁰ V. Sirotenko,⁵¹ P. Skubic,⁷⁶ P. Slattery,⁷² R.P. Smith,⁵¹ G.R. Snow,⁶⁸ J. Snow,⁷⁵ S. Snyder,⁷⁴ S. Söldner-Rembold,⁴⁵ X. Song,⁵³ L. Sonnenschein,¹⁷ A. Sopczak,⁴³ M. Sosebee,⁷⁹ K. Soustruznik,⁹ M. Souza,² B. Spurlock,⁷⁹ J. Stark,¹⁴ J. Steele,⁶¹ K. Stevenson,⁵⁵ V. Stolin,³⁷ A. Stone,⁵² D.A. Stoyanova,³⁹ J. Strandberg,⁴¹ M.A. Strang,⁷⁰ M. Strauss,⁷⁶ R. Ströhmer,²⁵ D. Strom,⁵⁴ M. Strovink,⁴⁷ L. Stutte,⁵¹ S. Sumowidagdo,⁵⁰ A. Sznajder,³ M. Talby,¹⁵ P. Tamburello,⁴⁶ W. Taylor,⁵ P. Telford,⁴⁵ J. Temple,⁴⁶ B. Tiller,²⁵ M. Titov,²³ V.V. Tokmenin,³⁶ M. Tomoto,⁵¹ T. Toole,⁶² I. Torchiani,²³ S. Towers,⁴³ T. Trefzger,²⁴ S. Trincz-Duvoid,¹⁷ D. Tsybychev,⁷³ B. Tuchming,¹⁸ C. Tully,⁶⁹ A.S. Turcot,⁴⁵ P.M. Tuts,⁷¹ R. Unalan,⁶⁶ L. Uvarov,⁴⁰ S. Uvarov,⁴⁰ S. Uzunyan,⁵³ B. Vachon,⁵ P.J. van den Berg,³⁴ R. Van Kooten,⁵⁵ W.M. van Leeuwen,³⁴ N. Varelas,⁵² E.W. Varnes,⁴⁶ A. Vartapetian,⁷⁹ I.A. Vasilyev,³⁹ M. Vaupel,²⁶ P. Verdier,²⁰ L.S. Vertogradov,³⁶ M. Verzocchi,⁵¹ F. Villeneuve-Seguié,⁴⁴ P. Vint,⁴⁴ J.-R. Vlimant,¹⁷ E. Von Toerne,⁶⁰ M. Voutilainen,^{68,†} M. Vreeswijk,³⁴ H.D. Wahl,⁵⁰ L. Wang,⁶² J. Warchol,⁵⁶ G. Watts,⁸³ M. Wayne,⁵⁶ M. Weber,⁵¹ H. Weerts,⁶⁶ N. Wermes,²² M. Wetstein,⁶² A. White,⁷⁹ D. Wicke,²⁶ G.W. Wilson,⁵⁹ S.J. Wimpenny,⁴⁹ M. Wobisch,⁵¹ J. Womersley,⁵¹ D.R. Wood,⁶⁴ T.R. Wyatt,⁴⁵ Y. Xie,⁷⁸ N. Xuan,⁵⁶ S. Yacoob,⁵⁴ R. Yamada,⁵¹ M. Yan,⁶² T. Yasuda,⁵¹ Y.A. Yatsunenko,³⁶ K. Yip,⁷⁴ H.D. Yoo,⁷⁸ S.W. Youn,⁵⁴ C. Yu,¹⁴ J. Yu,⁷⁹ A. Yurkewicz,⁷³ A. Zatserklyaniy,⁵³ C. Zeitnitz,²⁶ D. Zhang,⁵¹ T. Zhao,⁸³ Z. Zhao,⁶⁵ B. Zhou,⁶⁵ J. Zhu,⁷³ M. Zielinski,⁷² D. Zieminska,⁵⁵ A. Zieminski,⁵⁵ V. Zutshi,⁵³ and E.G. Zverev³⁸

(DØ Collaboration)

¹ Universidad de Buenos Aires, Buenos Aires, Argentina

² LAFEX, Centro Brasileiro de Pesquisas Físicas, Rio de Janeiro, Brazil

³ Universidade do Estado do Rio de Janeiro, Rio de Janeiro, Brazil

⁴ Instituto de Física Teórica, Universidade Estadual Paulista, São Paulo, Brazil

⁵ University of Alberta, Edmonton, Alberta, Canada, Simon Fraser University, Burnaby, British Columbia, Canada, York University, Toronto, Ontario, Canada, and McGill University, Montreal, Quebec, Canada

⁶ Institute of High Energy Physics, Beijing, People's Republic of China

⁷ University of Science and Technology of China, Hefei, People's Republic of China

⁸ Universidad de los Andes, Bogotá, Colombia

⁹ Center for Particle Physics, Charles University, Prague, Czech Republic

¹⁰ Czech Technical University, Prague, Czech Republic

¹¹ Center for Particle Physics, Institute of Physics, Academy of Sciences of the Czech Republic, Prague, Czech Republic

¹² Universidad San Francisco de Quito, Quito, Ecuador

¹³ Laboratoire de Physique Corpusculaire, IN2P3-CNRS, Université Blaise Pascal, Clermont-Ferrand, France

¹⁴ Laboratoire de Physique Subatomique et de Cosmologie, IN2P3-CNRS, Université de Grenoble 1, Grenoble, France

¹⁵ CPPM, IN2P3-CNRS, Université de la Méditerranée, Marseille, France

¹⁶ IN2P3-CNRS, Laboratoire de l'Accélérateur Linéaire, Orsay, France

¹⁷ LPNHE, IN2P3-CNRS, Universités Paris VI and VII, Paris, France

¹⁸ DAPNIA/Service de Physique des Particules, CEA, Saclay, France

¹⁹ IReS, IN2P3-CNRS, Université Louis Pasteur, Strasbourg, France, and Université de Haute Alsace, Mulhouse, France

²⁰ Institut de Physique Nucléaire de Lyon, IN2P3-CNRS, Université Claude Bernard, Villeurbanne, France

²¹ III. Physikalisches Institut A, RWTH Aachen, Aachen, Germany

²² Physikalisches Institut, Universität Bonn, Bonn, Germany

²³ Physikalisches Institut, Universität Freiburg, Freiburg, Germany

²⁴ Institut für Physik, Universität Mainz, Mainz, Germany

²⁵ Ludwig-Maximilians-Universität München, München, Germany

- ²⁶ *Fachbereich Physik, University of Wuppertal, Wuppertal, Germany*
- ²⁷ *Panjab University, Chandigarh, India*
- ²⁸ *Delhi University, Delhi, India*
- ²⁹ *Tata Institute of Fundamental Research, Mumbai, India*
- ³⁰ *University College Dublin, Dublin, Ireland*
- ³¹ *Korea Detector Laboratory, Korea University, Seoul, Korea*
- ³² *SungKyunKwan University, Suwon, Korea*
- ³³ *CINVESTAV, Mexico City, Mexico*
- ³⁴ *FOM-Institute NIKHEF and University of Amsterdam/NIKHEF, Amsterdam, The Netherlands*
- ³⁵ *Radboud University Nijmegen/NIKHEF, Nijmegen, The Netherlands*
- ³⁶ *Joint Institute for Nuclear Research, Dubna, Russia*
- ³⁷ *Institute for Theoretical and Experimental Physics, Moscow, Russia*
- ³⁸ *Moscow State University, Moscow, Russia*
- ³⁹ *Institute for High Energy Physics, Protvino, Russia*
- ⁴⁰ *Petersburg Nuclear Physics Institute, St. Petersburg, Russia*
- ⁴¹ *Lund University, Lund, Sweden, Royal Institute of Technology and Stockholm University, Stockholm, Sweden, and Uppsala University, Uppsala, Sweden*
- ⁴² *Physik Institut der Universität Zürich, Zürich, Switzerland*
- ⁴³ *Lancaster University, Lancaster, United Kingdom*
- ⁴⁴ *Imperial College, London, United Kingdom*
- ⁴⁵ *University of Manchester, Manchester, United Kingdom*
- ⁴⁶ *University of Arizona, Tucson, Arizona 85721, USA*
- ⁴⁷ *Lawrence Berkeley National Laboratory and University of California, Berkeley, California 94720, USA*
- ⁴⁸ *California State University, Fresno, California 93740, USA*
- ⁴⁹ *University of California, Riverside, California 92521, USA*
- ⁵⁰ *Florida State University, Tallahassee, Florida 32306, USA*
- ⁵¹ *Fermi National Accelerator Laboratory, Batavia, Illinois 60510, USA*
- ⁵² *University of Illinois at Chicago, Chicago, Illinois 60607, USA*
- ⁵³ *Northern Illinois University, DeKalb, Illinois 60115, USA*
- ⁵⁴ *Northwestern University, Evanston, Illinois 60208, USA*
- ⁵⁵ *Indiana University, Bloomington, Indiana 47405, USA*
- ⁵⁶ *University of Notre Dame, Notre Dame, Indiana 46556, USA*
- ⁵⁷ *Purdue University Calumet, Hammond, Indiana 46323, USA*
- ⁵⁸ *Iowa State University, Ames, Iowa 50011, USA*
- ⁵⁹ *University of Kansas, Lawrence, Kansas 66045, USA*
- ⁶⁰ *Kansas State University, Manhattan, Kansas 66506, USA*
- ⁶¹ *Louisiana Tech University, Ruston, Louisiana 71272, USA*
- ⁶² *University of Maryland, College Park, Maryland 20742, USA*
- ⁶³ *Boston University, Boston, Massachusetts 02215, USA*
- ⁶⁴ *Northeastern University, Boston, Massachusetts 02115, USA*
- ⁶⁵ *University of Michigan, Ann Arbor, Michigan 48109, USA*
- ⁶⁶ *Michigan State University, East Lansing, Michigan 48824, USA*
- ⁶⁷ *University of Mississippi, University, Mississippi 38677, USA*
- ⁶⁸ *University of Nebraska, Lincoln, Nebraska 68588, USA*
- ⁶⁹ *Princeton University, Princeton, New Jersey 08544, USA*
- ⁷⁰ *State University of New York, Buffalo, New York 14260, USA*
- ⁷¹ *Columbia University, New York, New York 10027, USA*
- ⁷² *University of Rochester, Rochester, New York 14627, USA*
- ⁷³ *State University of New York, Stony Brook, New York 11794, USA*
- ⁷⁴ *Brookhaven National Laboratory, Upton, New York 11973, USA*
- ⁷⁵ *Langston University, Langston, Oklahoma 73050, USA*
- ⁷⁶ *University of Oklahoma, Norman, Oklahoma 73019, USA*
- ⁷⁷ *Oklahoma State University, Stillwater, Oklahoma 74078, USA*
- ⁷⁸ *Brown University, Providence, Rhode Island 02912, USA*
- ⁷⁹ *University of Texas, Arlington, Texas 76019, USA*
- ⁸⁰ *Southern Methodist University, Dallas, Texas 75275, USA*
- ⁸¹ *Rice University, Houston, Texas 77005, USA*
- ⁸² *University of Virginia, Charlottesville, Virginia 22901, USA*
- ⁸³ *University of Washington, Seattle, Washington 98195, USA*

(Dated: May 15, 2006)

We present the results of a search for a new particle X produced in $p\bar{p}$ collisions at $\sqrt{s} = 1.96$ TeV and subsequently decaying to $Z\gamma$. The search uses 0.3 fb^{-1} of data collected with the DØ

detector at the Fermilab Tevatron Collider. We set limits on the production cross section times the branching fraction $\sigma(p\bar{p} \rightarrow X) \times B(X \rightarrow Z\gamma)$ that range from 0.4 to 3.5 pb at the 95% C.L. for X with invariant masses between 100 and 1000 GeV/ c^2 , over a wide range of X decay widths.

There is considerable evidence that the standard model (SM) is incomplete [1]. Signs of new physics may appear in the form of a new particle (X). If X is a scalar, pseudo-scalar, or tensor, its decay to lepton pairs might be highly suppressed, but it could have a large decay branching fraction (B) to the di-boson final state $Z\gamma$. A search for X in the $Z\gamma$ final state thus complements previous searches (for example [2]) for production of a new vector boson in the lepton pair decay mode.

Events with pairs of vector bosons have been studied as tests of the SM of electroweak interactions. Specifically, the Z plus photon final state ($Z\gamma$) has been investigated by the DØ [3, 4] and CDF [5] collaborations using $p\bar{p}$ collisions and by the LEP collaborations [6, 7, 8] using e^+e^- collisions. In these cases, the measured cross section and photon energy distribution were used to set limits on anomalous Z -photon couplings, but no explicit searches for new particles decaying to $Z\gamma$ were performed. The L3 Collaboration [9] searched for Higgs boson production, with subsequent decay of the Higgs to $Z\gamma$, in electron-positron collisions at the LEP2 collider, and set cross section limits for Higgs boson masses up to 190 GeV/ c^2 .

In the SM, the dilepton plus γ final state, including $Z\gamma$, is expected to be produced through radiative processes (Figs. 1a and b). In addition, this final state is also expected from Higgs boson production and decay (Fig. 1c). Although the Higgs boson mass is unknown and the predicted $H \rightarrow Z\gamma$ branching fraction is $\mathcal{O}(10^{-3})$, extensions to the SM can significantly increase this branching fraction [10, 11, 12, 13]. Other SM extensions predict new particles that decay into $Z\gamma$. For example, a Z' boson can decay radiatively to a Z boson and a photon [14]. In models with a fourth generation of fermions, a top and anti-top quark bound state (toponium) may exist [15, 16], and this state can decay to $Z\gamma$. In theories with compact extra dimensions, massive Kaluza-Klein spin-2 gravitons can also decay to the $Z\gamma$ final state [17]. The presence of resonance behavior in the $Z\gamma$ final state can thus signal the presence of a wide variety of new physics. In order to make quantitative statements, we will assume that this new physics manifests itself in the form of a spin 0 particle.

A large sample of $Z\gamma$ events has been collected by the DØ experiment and analyzed to measure the $Z\gamma$ cross section and set limits on anomalous $ZZ\gamma$ and $Z\gamma\gamma$ couplings [3]. The Fermilab Tevatron Collider provides a higher energy reach than that available to previous experiments, and so this sample deserves further scrutiny. Experimentally, Z bosons are identified through their decay to charged lepton pairs ($\ell\ell = ee$ or $\mu\mu$). Photons are measured with high precision from their electromagnetic

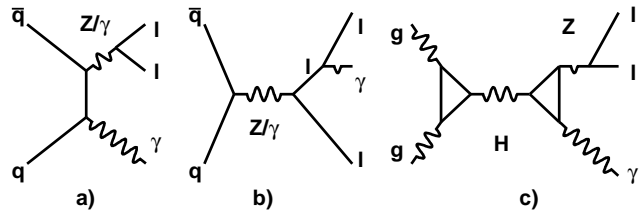


FIG. 1: The Feynman diagrams for standard model sources of dilepton plus γ events are shown. Diagram a) shows $q\bar{q} \rightarrow Z$ -boson plus γ , where the photon is radiated from the quark or anti-quark. Diagram b) shows $q\bar{q} \rightarrow Z/\gamma$, where the photon is radiated from one of the Z boson's decay products. Diagram c) shows Higgs production and decay into a Z boson and a photon.

showers. The $Z\gamma$ final state has small backgrounds. We focus on, by tightening kinematic selection criteria, and study the mass distribution of the $\ell\ell\gamma$ events in a sample of 0.3 fb^{-1} of $p\bar{p}$ collision data collected with the DØ Run II detector from April 2002 to June 2004 at the Fermilab Tevatron Collider at $\sqrt{s} = 1.96 \text{ TeV}$.

The DØ detector [18] includes a central tracking system, composed of a silicon microstrip tracker and a central fiber tracker, both located within a 2 T superconducting solenoidal magnet and optimized for tracking and vertexing capability at pseudorapidities [19] of $|\eta| < 2.5$. Three liquid argon and uranium calorimeters provide coverage up to $|\eta| \approx 4.2$: a central section, and two end calorimeters. A muon system resides beyond the calorimetry, and consists of tracking detectors, scintillation counters, and a 1.8 T toroid with coverage for $|\eta| < 2$. Luminosity is measured using scintillator arrays located in front of the end calorimeter cryostats, covering $2.7 < |\eta| < 4.4$. Trigger and data acquisition systems are designed to accommodate the high luminosities of the Run II Tevatron.

The analysis is conducted in two channels, one where the Z boson decays into electrons and the other where it decays into muons. Electron candidate events are required to satisfy one of a series of single electron triggers. The electron channel requires that electron candidates be isolated in the calorimeter, have longitudinal and transverse energy deposition profiles consistent with those of an electron, have a transverse momentum $p_T > 15 \text{ GeV}/c$, and be contained in either the central calorimeter (CC, $|\eta| < 1.1$) or one of the end calorimeters (EC, $1.5 < |\eta| < 2.5$) and not in the transition region between the central and the end calorimeters. If an electron candidate is in the CC, it is required to have a spatially matched track from the central tracker. One of the elec-

trons must have $p_T > 25$ GeV/ c . The efficiency for a di-electron candidate to satisfy the trigger and for both electrons to satisfy all quality requirements lead to an event efficiency of 0.69 ± 0.05 if both electrons are in the CC and 0.78 ± 0.05 if one electron is in the EC. Events with both electron candidates in the EC are not considered due to a small expected number of events from X and large backgrounds. These efficiencies are measured with the inclusive Z boson candidate events.

Muon candidate events must pass one of a suite of single or di-muon triggers. The muon channel requires two candidate muons with $p_T > 15$ GeV/ c and opposite charge. Both muons must be matched to tracks found in the central tracker. The background from heavy flavor production is suppressed by requiring the muon candidates to be isolated. The background from cosmic rays is suppressed by requiring that the muons come from the interaction region and are not exactly back-to-back. The efficiency for di-muon event selection and trigger is 0.84 ± 0.05 per event. This efficiency is measured with Z boson candidate events.

Photon candidates must be isolated in the calorimeter and tracker, have longitudinal and transverse shapes in the calorimeter consistent with those of a photon, have $p_T > 25$ GeV/ c , and be contained in the central calorimeter ($|\eta| < 1.1$). The efficiency is around 0.85 at 25 GeV/ c and rises to a plateau of 0.90 at 35 GeV/ c .

Both di-electron and di-muon candidate events are further required to have a di-lepton mass greater than 75 GeV/ c^2 , and a photon separated from both leptons by $\Delta\mathcal{R} > 0.7$ [20]. These requirements reduce the contribution from events in which a final state lepton radiates a photon. The detector acceptance times particle identification and trigger efficiency, for all requirements described, rises from about 18% to about 20% for masses from 100 to 800 GeV/ c^2 and at higher masses decrease. At mass greater than 800 GeV/ c^2 , a significant number of leptons fall within the isolation region of the other lepton, and charge misidentification becomes significant. The uncertainty on these are the dominant contributors to the systematic uncertainty on the expected number of signal candidates. At 800 GeV/ c^2 , the uncertainty is approximately 10% and at 1000 GeV/ c^2 , the uncertainty has risen to 40%.

To improve the di-lepton-photon mass resolution in the muon channel, the muon transverse momenta are adjusted by employing a one-constraint kinematic fit that forces the di-muon mass to equal the on-shell Z -boson mass. This constraint is only enforced if the fit has $\chi^2/\text{d.o.f.} < 7$. Monte Carlo studies show this technique improves the three-body mass resolution from 6.7% to 3.4%, which is comparable to the mass resolution of the electron channel, 3.9% obtained without a kinematic fit. For the $Z\gamma$ mass range considered, photon energy contributions to the three-body mass resolution is much larger than that of the Z boson width, which is neglected in the

kinematic fit.

Backgrounds to $Z\gamma$ production from the decay of a new particle include the SM $Z\gamma$ and Z +jet processes, where the jet is misidentified as a photon. Backgrounds from processes with a photon where one or both of the leptons is due to a misidentified jet are found to be negligible. Contributions from $Z\gamma$ events with $Z \rightarrow \tau\tau$ and subsequent leptonic decays of the tau are less than 1% of the sample. Contributions from WZ and ZZ processes, where electrons are misidentified as photons, are also less than 1% of the sample.

Efficiencies and background contributions are calculated using independent data samples and Monte Carlo simulations. Scalar particle decays to $Z\gamma$ are modeled using PYTHIA [21] SM Higgs boson production in which the Higgs boson is forced to decay to $Z\gamma$, and the Z boson is forced to decay into leptons. For the SM $Z\gamma$ events, we use an event generator employing first-order QCD calculations and first-order EW radiation [22]. These events are processed through a parameterized detector simulation that is tuned on Z boson candidate events. The background due to jets misidentified as photons is estimated by scaling the measured Z +jet event rate by the measured probability for a jet to mimic a photon [3].

The final sample used in the analysis consists of 13 candidates in the electron channel and 15 candidates in the muon channel. We expect from SM sources 11.2 ± 0.8 events in the electron channel and 12.9 ± 0.9 events in the muon channel. Approximately 75% of the expected SM contribution is due to SM $Z\gamma$. Uncertainties in the SM contributions are due to uncertainties in the luminosity, higher order QCD contributions, parton distribution functions, and the rate at which a jet mimics a photon. The luminosity uncertainty is the largest: 0.5 events for the electron channel and 0.7 events for the muon channel. In Fig 2 we plot the three-body mass against the two-body mass for the candidates. The muon candidates are shown before the two-body mass constraint is applied. A single candidate fails the χ^2 cut for this constraint; it is the candidate with $M_{ll} = 76$ GeV/ c^2 and $M_{ll\gamma} = 107$ GeV/ c^2 . The $M_{ll\gamma}$ spectrum of the electron and muon data samples individually are consistent with the shapes of their respective Monte Carlo samples. The three-body mass, $M_{ll\gamma}$, of the combined sample is shown in Fig. 3. The SM expectations are also shown together with those for a 130 GeV/ c^2 scalar decaying into $Z\gamma$ with $\sigma \times B$ of 1 pb. This figure is just for illustration purposes and is not used further in the analysis.

None of the 28 candidate events has more than one photon or more than two leptons. Among all the events we only find three jets with $p_T > 15$ GeV/ c . Two of these jets are in a single event. The missing transverse momentum in all candidate events is less than 20 GeV/ c .

We use two methods in our search to ensure sensitivity to scalar states over a broad range of natural decay widths. The first looks for an excess in a sliding narrow

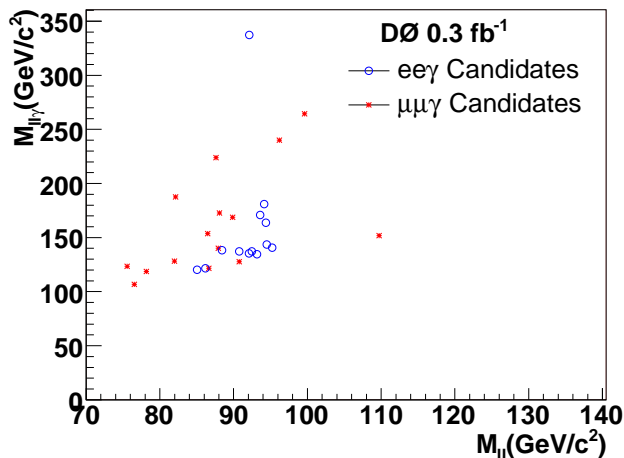


FIG. 2: Distribution of candidates in the three-body mass, $M_{ll\gamma}$, vs two-body mass, M_{ll} , plane is shown. The electron candidates are blue circles and the muons are red stars. The muon candidates are shown before the two-body mass constraint is applied.

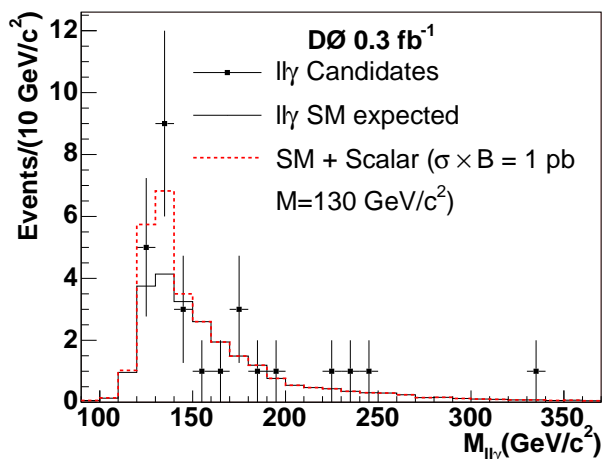


FIG. 3: Distribution of the three-body mass, $M_{ll\gamma}$, for candidate events and SM expectations. The signal shape for a 130 GeV/c^2 scalar decaying to $Z\gamma$ with a $\sigma(p\bar{p} \rightarrow X) \times B(X \rightarrow Z\gamma) = 1$ pb is also shown.

window in the $M_{ll\gamma}$ spectrum, while the second sets a sliding lower mass threshold and counts events above this threshold. The window technique gives very good separation of signal from background; however it is sensitive to the natural width (Γ) of the new particle. The separation of signal from background of the window method is highest when Γ is small compared to the mass resolution. The size of the search window was chosen to be 4.4% of the mass by optimization of the signal MC acceptance for a 130 GeV/c^2 $Z\gamma$ resonance over the square-root of the SM background expectation.

The threshold technique also generally requires knowl-

edge of Γ . To reduce this dependence, we place the threshold at the median value of the mass distribution (M'), which introduces an acceptance factor of 0.5. The value of M' is the same as the nominal mass of the particle if its width is fairly narrow ($\lesssim 4 \text{ GeV}/c^2$), or if its mass is fairly low ($\lesssim 250 \text{ GeV}/c^2$). If neither condition is met, the available parton luminosity begins to affect the generated mass distribution. The SM Higgs boson provides a good example of this effect. A Higgs with a nominal mass of 250 GeV/c^2 has a width of 4 GeV/c^2 and the median mass is 249.7 GeV/c^2 . As the nominal mass increases, the width grows and the median mass begins to deviate from the nominal value. At 350 and 450 GeV/c^2 , the widths are 15 and 42 GeV/c^2 , respectively; and the median masses are 346.4 and 401.0 GeV/c^2 , respectively.

Using these techniques, we determine the agreement between data and SM expectations, taking into account systematic uncertainties. Using the threshold technique, we find that the smallest probability of agreement between data and SM expectations is 7%, which occurs at the median mass $M' = 230 \text{ GeV}/c^2$. Applying the narrow mass window method to search for objects with $\Gamma \rightarrow 0$ (i.e. generated within the mass bin), we find that for a mass of 140 GeV/c^2 , the probability of agreement between the data and SM expectation is 0.8%. The window at 140 GeV/c^2 has the lowest probability of agreement in the mass range considered. To further assess the statistical significance of this effect, we generate an ensemble of 100,000 simulated experiments in which only SM sources for $Z\gamma$ were included and possible systematic effects are neglected. Eleven percent of the experiments contain a search window with a probability of agreement with the SM expectation of 0.5% or less. The disagreement of 140 GeV/c^2 mass window has a significance of less than 2.5 standard deviations and lies at the mass where the SM background is largest and, therefore, where the ensemble tests indicate fluctuations would also be largest.

Since we find no excess in the data compared to the SM expectation, we extract limits on $\sigma(p\bar{p} \rightarrow X) \times B(X \rightarrow Z\gamma)$ for new scalar states. The limits are set using a Bayesian technique [23] with a flat prior for the signal and with systematic uncertainties on the signal and background taken into account.

We extract the sensitivity and limits for two cases. In the first case, Fig. 4, we use the window technique and assume the width is negligible compared to the detector resolution. In the second case, Fig. 5, we use the threshold technique where the width is allowed to be at the other extreme. The expected limit for the window technique is less stringent where SM sources provide the largest number of events; it is more stringent between 300 and 800 GeV/c^2 where no events are expected; it finally rises with mass as efficiency decreases and the systematic uncertainties increase. We see qualitatively similar structures from the threshold technique limit. In comparing

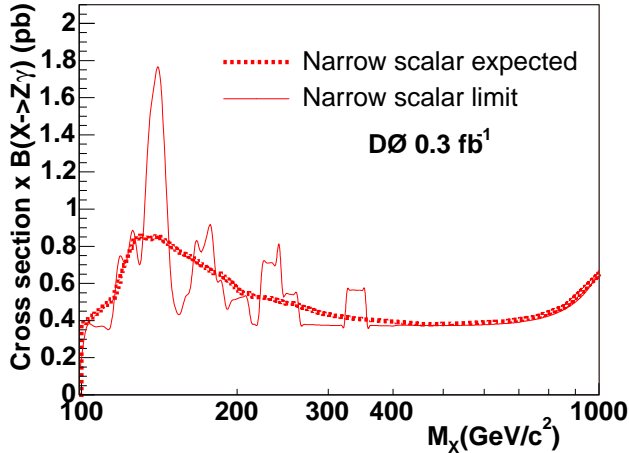


FIG. 4: The expected and observed cross section times branching fraction 95% C.L. limit for a scalar X decaying into $Z\gamma$ as a function of M for narrow scalar.

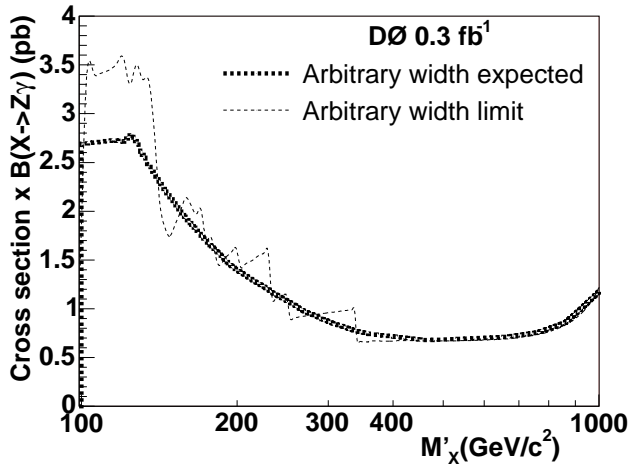


FIG. 5: The expected and observed cross section times branching fraction 95% C.L. limit for a scalar X decaying into $Z\gamma$ as a function of M' for wide scalar. M' is the median of the true mass distribution for a generic object using the arbitrary width technique.

the two limits it should be noted that M' is lower than the nominal mass of the particle. In Fig. 6, curves representing the expected cross section times branching fraction for three Higgs models are compared to the limits. These models are the SM Higgs boson [10], a fermiophobic Higgs boson [12], and a model with four generations of quarks [13].

In summary, we have performed the first search for $Z\gamma$ resonant states at a hadron collider with an invariant mass greater than $100 \text{ GeV}/c^2$. We find no statistically significant evidence for the existence of these objects. Narrowing our search to scalar and pseudo-scalar resonances, we limit the production cross section times

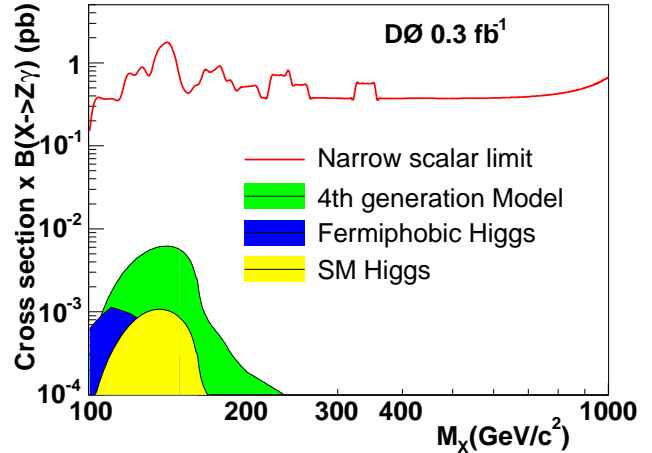


FIG. 6: The cross section times branching fraction 95% C.L. limits for a narrow scalar X decaying into $Z\gamma$ as a function of M . Curves representing the cross section times branching ratio expected from three variations of the Higgs are shown.

branching fraction to less than 0.4 to 3.5 pb depending on the mass and width.

We thank the staffs at Fermilab and collaborating institutions, and acknowledge support from the DOE and NSF (USA); CEA and CNRS/IN2P3 (France); FASI, Rosatom and RFBR (Russia); CAPES, CNPq, FAPERJ, FAPESP and FUNDUNESP (Brazil); DAE and DST (India); Colciencias (Colombia); CONACyT (Mexico); KRF and KOSEF (Korea); CONICET and UBACyT (Argentina); FOM (The Netherlands); PPARC (United Kingdom); MSMT (Czech Republic); CRC Program, CFI, NSERC and WestGrid Project (Canada); BMBF and DFG (Germany); SFI (Ireland); The Swedish Research Council (Sweden); Research Corporation; Alexander von Humboldt Foundation; and the Marie Curie Program.

[*] On leave from IEP SAS Kosice, Slovakia.

[†] Visitor from Helsinki Institute of Physics, Helsinki, Finland.

- [1] C. Quigg, eConf **C040802**, L001 (2004) [arXiv:hep-ph/0502070]; and references therein.
- [2] D. Feldman, Z. Liu and P. Nath, arXiv:hep-ph/0603039.
- [3] DØ Collaboration, V. M. Abazov *et al.*, Phys. Rev. Lett. **95**, 051802 (2005).
- [4] DØ Collaboration, B. Abbott *et al.*, Phys. Rev. D **57**, 3817 (1998); DØ Collaboration, S. Abachi *et al.*, Phys. Rev. Lett. **78**, 3640 (1997); DØ Collaboration, S. Abachi *et al.*, Phys. Rev. Lett. **75**, 1028 (1995).
- [5] CDF II Collaboration, D. Acosta *et al.*, Phys. Rev. Lett. **94**, 041803 (2005); CDF Collaboration, F. Abe *et al.*, Phys. Rev. Lett. **74**, 1941 (1995).
- [6] DELPHI Collaboration, P. Abreu *et al.*, Phys. Lett. B

- 423**, 194 (1998).
- [7] L3 Collaboration, P. Achard *et al.*, Phys. Lett. B **597**, 119 (2004).
- [8] OPAL Collaboration, G. Abbiendi *et al.*, Eur. Phys. J. C **17**, 553 (2000).
- [9] L3 Collaboration, P. Achard *et al.*, Phys. Lett. B **589**, 151 (2004).
- [10] M. Spira, Report DESY T-95-05 (October 1995), arXiv:hep-ph/9510347.
- [11] V. Büscher and K. Jakobs, Int. J. Mod. Phys. A **20**, 2523 (2005).
- [12] A. G. Akeroyd, A. Alves, M. A. Diaz and O. J. P. Eboli, arXiv:hep-ph/0512077; A. Alves, private communications for $\tan\beta = 30$ and a charged Higgs mass of 100 GeV.
- [13] E. Arik, O. Cakir, S. A. Cetin and S. Sultansoy, Phys. Rev. D **66**, 033003 (2002).
- [14] G. A. Kozlov, Phys. Rev. D **72**, 075015 (2005).
- [15] S. Ono, Acta Phys. Polon. B **15**, 201 (1984).
- [16] O. Cakir, R. Ciftci, E. Recepoglu, and S. Sultansoy, Acta Phys. Polon. B **35**, 2103 (2004).
- [17] H. Davoudiasl, J. L. Hewett, and T. G. Rizzo, Phys. Rev. D **63**, 075004 (2001)
- [18] V. Abazov *et al.*, accepted for publication by Nucl. Instrum. Methods A, arXiv:physics/0507191.
- [19] We use a cylindrical coordinate system about the beamline in which positive z is along the proton direction, θ is the polar angle, ϕ is the azimuthal angle, and pseudorapidity (η) is defined as $\eta = -\ln[\tan(\theta/2)]$.
- [20] In the $D\bar{O}$ coordinate system $\Delta\mathcal{R} = \sqrt{(\Delta\phi_{\ell\gamma})^2 + (\Delta\eta_{\ell\gamma})^2}$.
- [21] T. Sjöstrand *et al.*, Computer Physics Commun. **135**, 238 (2001). Version 6.2.
- [22] U. Baur and E. Berger, Phys. Rev. D **47**, 4889 (1993).
- [23] R.T. Cox, Am. J. Phys. **14**, 1 (1946); H. Jeffreys, "Theory of Probability," 3rd edition, Oxford University Press, (1961).